

## The absorption rate of CO<sub>2</sub>/SO<sub>2</sub>/NO<sub>2</sub> into a blended aqueous AMP/ammonia solution

Jong-Beom Seo\*, Soo-Bin Jeon\*, Won-Joon Choi\*\*, Jae-Won Kim\*\*\*, Gou-Hong Lee\*\*\*\*, and Kwang-Joong Oh\*†

\*Department of Environmental Engineering and Pusan National University, Busan 609-735, Korea

\*\*Greenhouse Gas Research Center and Korea Institute of Energy Research, Daejeon 305-343, Korea

\*\*\*DONGKUK STEEL MILL CO., LTD, Gyeongbuk 790-729, Korea

\*\*\*\*Environmental Management Division Ulsan Metropolitan City, Gyeongnam 680-701, Korea

(Received 23 February 2010 • accepted 24 May 2010)

**Abstract**—The Inter-governmental Panel on Climate Change (IPCC) reported that human activities result in the production of greenhouse gases (CO<sub>2</sub>, CH<sub>4</sub>, N<sub>2</sub>O and CFCs), which significantly contribute to global warming, one of the most serious environmental problems. Under these circumstances, most nations have shown a willingness to suffer economic burdens by signing the Kyoto Protocol, which took effect from February 2005. Therefore, an innovative technology for the simultaneous removal carbon dioxide (CO<sub>2</sub>) and nitrogen dioxide (NO<sub>2</sub>), which are discharged in great quantities from fossil fuel-fired power plants and incineration facilities, must be developed to reduce these economical burdens. In this study, a blend of AMP and NH<sub>3</sub> was used to achieve high absorption rates for CO<sub>2</sub>, as suggested in several publications. The absorption rates of CO<sub>2</sub>, SO<sub>2</sub> and NO<sub>2</sub> into aqueous AMP and blended AMP+NH<sub>3</sub> solutions were measured using a stirred-cell reactor at 293, 303 and 313 K. The reaction rate constants were determined from the measured absorption rates. The effect of adding NH<sub>3</sub> to enhance the absorption characteristics of AMP was also studied. The performance of the reactions was evaluated under various operating conditions. From the results, the reactions with SO<sub>2</sub> and NO<sub>2</sub> into aqueous AMP and AMP+NH<sub>3</sub> solutions were classified as instantaneous reactions. The absorption rates increased with increasing reaction temperature and NH<sub>3</sub> concentration. The reaction rates of 1, 3 and 5 wt% NH<sub>3</sub> blended with 30 wt% AMP solution with respect to CO<sub>2</sub>/SO<sub>2</sub>/NO<sub>2</sub> at 313 K were 6.05–8.49 × 10<sup>-6</sup>, 7.16–10.41 × 10<sup>-6</sup> and 8.02–12.0 × 10<sup>-6</sup> kmol m<sup>-2</sup> s<sup>-1</sup>, respectively. These values were approximately 32.3–38.7% higher than with aqueous AMP solution alone. The rate of the simultaneous absorption of CO<sub>2</sub>/SO<sub>2</sub>/NO<sub>2</sub> into aqueous AMP+NH<sub>3</sub> solution was 3.83–4.87 × 10<sup>-6</sup> kmol m<sup>-2</sup> s<sup>-1</sup> at 15 kPa, which was an increase of 15.0–16.9% compared to 30 wt% AMP solution alone. This may have been caused by the NH<sub>3</sub> solution acting as an alternative for CO<sub>2</sub>/SO<sub>2</sub>/NO<sub>2</sub> controls from flue gas due to its high absorption capacity and fast absorption rate.

**Key words:** Carbon Dioxide, Sulfur Dioxide, Nitrogen Dioxide, Blended Gas, Simultaneous Absorption, 2-Amino-2-methyl-1-propanol, Ammonia

### INTRODUCTION

According to the United Nations Framework Convention on Climate Change (UNFCCC) in Kyoto, a commitment to reduce CO<sub>2</sub> emissions by 6% below 1990 levels was made by several countries. Industrialized countries, who should take the lead in combating climate change and its adverse effects [1] because they have been responsible for the majority of historical cumulative emissions, therefore were given quantified obligations to reduce emissions in the Kyoto Protocol [2].

Recently, the State of World Forum (2009.8), held in Brazil Belo Horizonte, decided to reduce 80% of greenhouse gas emissions by 2020 in the Global 2020 Climate Leadership Campaign. There are various technologies being used to separate CO<sub>2</sub> from the flue gas of conventional fossil fuel fired power plants: chemical absorption, physical absorption, cryogenic methods, membrane separation and biological fixation [3]. The chemical absorption process is generally recognized as the most effective technology [4].

Aqueous MEA solution is the most frequently used alkanola-

mines absorbent, owing to its high reactivity with CO<sub>2</sub>, low solvent cost and ease of regeneration [5]. However, the maximum CO<sub>2</sub> absorption capacity in MEA is limited by the stoichiometry to 0.5 mol CO<sub>2</sub>/mol amine. A different class of chemical absorbents, sterically hindered amines, such as 2-amino-2-methyl-1-propanol (AMP), have been proposed as commercially attractive new CO<sub>2</sub> absorbent because of their advantages in absorption capacity, absorption rate, degradation resistance and ease of regeneration [6].

Previous investigations have shown that the CO<sub>2</sub> absorption load capacity of ammonia was twice that of AMP, with a much enhanced removal efficiency over that of MEA, the use of an anti-bubbling is also not required and AMP is much cheaper than MEA. It is also expected that AMP will be able to complement the weak point of the excessive energy consumption and the corrosion of reactor during the regeneration process of MEA.

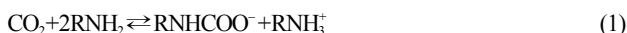
Consequently, this study hopes to show that the addition of ammonia, which has excellent absorption efficiencies for CO<sub>2</sub>, SO<sub>2</sub> and NO<sub>2</sub>, will improve the AMP absorption ratio. The simultaneous absorption rates of CO<sub>2</sub>/SO<sub>2</sub>/NO<sub>2</sub> on the addition of NH<sub>3</sub> into aqueous AMP solutions were measured using a plane agitation absorption reactor, with the results compared with those for AMP alone. The performances were evaluated under various operating condi-

†To whom correspondence should be addressed.  
E-mail: kjoh@pusan.ac.kr

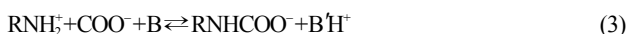
tions in order to investigate the absorption characteristics of the absorbents for the removal of CO<sub>2</sub>/SO<sub>2</sub>/NO<sub>2</sub>.

## THEORETICAL BACKGROUND

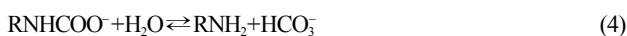
The following reactions occur with CO<sub>2</sub> in aqueous solutions of primary alkanolamines [7].



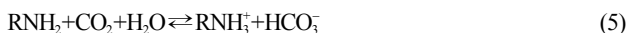
The Zwitterion mechanism originally proposed by Caplow [8], and reintroduced by Danckwerts [7], is generally accepted as the mechanism for reaction (1).



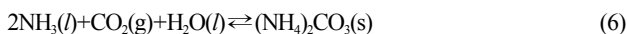
This mechanism is comprised of two steps: the reaction for the formation of the CO<sub>2</sub>-amine Zwitterion, followed by base-catalyzed deprotonation of this Zwitterion [reaction (3)]. Here B' is a base, which could be an amine, OH, or H<sub>2</sub>O [9]. The equilibrium loading capacities of primary and secondary alkanolamines are limited by the stoichiometry of reaction (1) to 0.5 mol of CO<sub>2</sub>/mol of amine. For normal primary amines, such as monoethanolamine (MEA), the carbamate formed from reaction (1) is quite stable. If the carbamate is unstable, as in the case of a hindered amine carbamate, such as AMP, it undergoes carbamate reversible reaction, as follows [10]:



Reaction (4) indicates that 1 mol of CO<sub>2</sub> is absorbed per 1 mol of hindered amine. However, a certain amount of carbamate hydrolysis [reaction (4)] occurs with all amines; therefore, the CO<sub>2</sub> loading may exceed stoichiometry (0.5), even with MEA, particularly at high pressures. Another alternative mechanism for the bicarbonate formation has been proposed by Chakraborty et al. [11].



The chemical reactions between CO<sub>2</sub> and NH<sub>3</sub> can be expressed by the following reactions [12,13]:

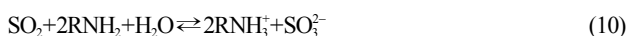


The wet method of ammonia scrubbing into flue gas to capture CO<sub>2</sub> produces ammonium carbonate ((NH<sub>4</sub>)<sub>2</sub>CO<sub>3</sub>) and ammonium bicarbonate (NH<sub>4</sub>HCO<sub>3</sub>) [14].

The chemical reactions between SO<sub>2</sub> and AMP are based on the assumption that the SO<sub>2</sub> combines with water [15] in an aqueous alkali solution [16]. The reaction is as follows:

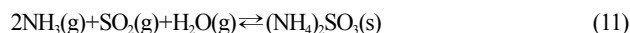


The overall reaction of amine-SO<sub>2</sub> is as follows:

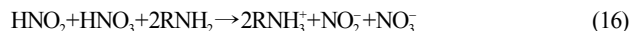
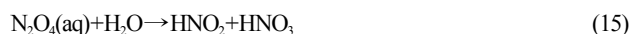


In addition, NH<sub>3</sub> absorbs SO<sub>2</sub> according to Eqs. (11) and (12) at room temperature and atmospheric pressure. The ammonium sulfite ((NH<sub>4</sub>)<sub>2</sub>

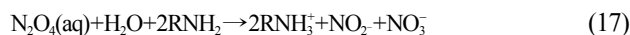
SO<sub>3</sub>) and ammonium bisulfite (NH<sub>4</sub>HSO<sub>3</sub>) are formed by reacting NH<sub>3</sub> with SO<sub>2</sub> [17].



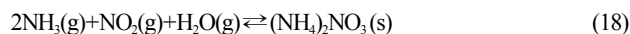
The reaction between NO<sub>2</sub> and AMP is assumed to be based on the combination with water and aqueous nitric acid solution.



Reaction (17) indicates the reaction for the generalization of N<sub>2</sub>O<sub>4</sub> from Eqs. (13)-(16)



In addition, ammonia absorbs NO<sub>2</sub> via reactions (18)-(19) at room temperature and atmospheric pressure.



For a chemical reaction between a gaseous constituent A and a liquid reactant B in an aqueous solution to yield a product P:



It is generally accepted that the Zwitterion mechanism governs the formation of a carbamate from primary and secondary amines. The first step in the reaction of CO<sub>2</sub> with AMP is the formation of an intermediate Zwitterion:



On the basis of the Zwitterion mechanism and the assumption of quasi-steady state for the concentration of the Zwitterion, the expression for the CO<sub>2</sub> reaction rate is as follows:

$$r_A = \frac{k_2[\text{CO}_2][\text{RNH}_2]}{1 + k_{-1}/\sum k_b[\text{B}]} \quad (22)$$

When the term  $k_{-1}/\sum k_b[\text{B}] \ll 1$ , the analysis is simplified to second-order kinetics, and the following equation can be used:

$$r_A = k_2[\text{CO}_2][\text{RNH}_2] \quad (23)$$

The influence on the absorption kinetics of all the chemical reactions between dissolved CO<sub>2</sub> and the reactants in solution is usually expressed by an "enhancement factor", E, over physical absorption [18]:

$$N_A = Bk_L C_A^+ \quad (24)$$

where E is a function of the Hatta number ( $H_u$ ) and the instantaneous reaction enhancement factor ( $E_i$ ) is defined as follows:

$$H_u = \left( \frac{2}{m+1} D_A k_{mn} (C_A^+)^{m-1} C_B^n \right)^{1/2} / k_L \quad (25)$$

$$E_i = \left( \frac{D_A}{D_B} \right)^{1/2} + \left( \frac{D_B}{D_A} \right)^{1/2} \frac{C_B}{\nu C_A^+} \quad (26)$$

where  $C_A^*$  is the concentration of the gas at the interface given by Henry's law:

$$C_A^* = p_A / H_A \quad (27)$$

The experimental conditions were selected to ensure the absorption of  $\text{CO}_2$  into amine solutions in a region of fast pseudo  $m$ -order reaction was in the range of  $H_u$  between 3 and  $E_i$ . If the value of  $H_u$  is within this range,  $E$  becomes equal to  $H_{u0}$  and the following specific absorption rate is obtained [18,19]:

$$N_A = \left( \frac{p_A}{H_A} \right)^{(m+1)/2} \left( \frac{2}{m+1} D_A k_{mn} C_B^n \right)^{1/2} \quad (28)$$

The slope of the straight line fitting the data of  $\ln$  versus  $\ln$  will give an order of  $m$  with respect to the dissolved gas concentration. The order of  $n$  with respect to the amine concentration can also be found in an analogous manner by plotting versus  $\ln$ . For a fast chemical reaction between the dissolved gas and a reactant, the specific absorption rate is as follows [18-21]:

$$N_A = C_A^* \sqrt{D_A k_{ov}} \quad (29)$$

Similarly, using reaction 30, the overall reaction rate ( $k_{ov}$ ) can be calculated, as follows:

$$k_{ov} = k_{mn} = (N_A H_A^{(m+1)/2} / p_A^{(m+1)/2} / D_A^{1/2})^2 \quad (30)$$

For fast pseudo- $m$ -order reaction conditions, when the equilibrium pressure of  $\text{CO}_2$  contributed by the  $\text{CO}_2$  in solutions is small compared to the absorption pressure, and where the gas phase resistance is negligible, the absorption rate is given by reaction 31 [15,16]. After integrating reaction 28, a reaction rate constant ( $k_2$ ) can be achieved from reaction 29.

$$-\frac{V_A}{RT} \left( \frac{dP_A}{dt} \right) = A_s \sqrt{D_A k_{ov}} \left( \frac{P_A}{H_A} \right) \quad (31)$$

$$-\left( \frac{dn}{dt} \right) = A_s \sqrt{D_A k_{ov}} C_A^* \quad (32)$$

$$\left( \frac{N_A H_A}{\sqrt{D_A P_A}} \right)^2 = k_{ov} \quad (33)$$

$$\left( \frac{N_A H_A}{\sqrt{D_A P_A}} \right)^2 = k_2 C_B \quad (34)$$

## EXPERIMENTAL MATERIALS AND METHODS

### 1. Materials

Analytical grade AMP solution, with a purity of 99%, was supplied by Acros Organics. A 28 wt% ammonia solution was supplied by Junsei Chemical. Aqueous solutions were prepared with distilled water. The  $\text{CO}_2$  and  $\text{N}_2$  gases were of commercial grade, with purities of 99.99%.

### 2. Absorption Rate Measurement

The experimental apparatus for measuring the absorption rate is shown in Fig. 1. The reactor, with a height of 160 mm and i.d. of 95 mm, was located inside a temperature-controlled vessel, with four 5-mm-wide glass plates adhering to the inner wall of the reactor to act as baffles. The total volume of the reactor was about 1,134  $\text{cm}^3$ , with an active interface area ( $A_s$ ) of 70.88  $\text{cm}^2$ . A two-blade impeller (70 mm  $\times$  20 mm) was installed in the middle of the liquid

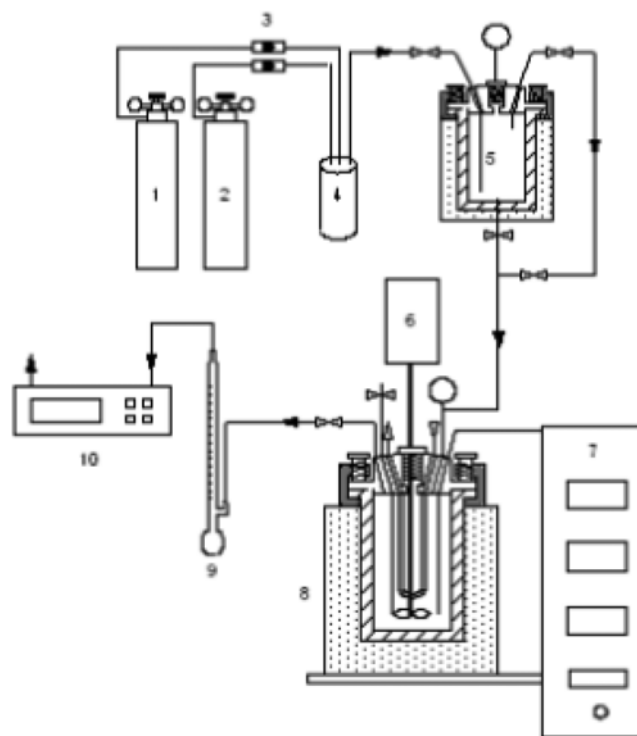


**Fig. 1. Schematic diagram of the experimental apparatus for measurement of the absorption rate.**

- |   |  |
|---|--|
| 1. $\text{N}_2$ cylinder                                      | 6. Magnetic drive                              |
| 2. $\text{CO}_2$ , $\text{SO}_2$ , and $\text{NO}_2$ cylinder | 7. Controller of temperature and stirrer speed |
| 3. Mass flow controller                                       | 8. Reactor (Agitated vessel)                   |
| 4. Mixing chamber   | 9. Soap film flow meter                        |
| 5. Saturator  | 10. Analyzer                                   |

level. The reactor temperature was measured by a K-type thermocouple, with an accuracy of 0.1 K. Pressure transducers (MGI/MGAMP series, with an accuracy of 0.1 kPa), were installed in the reactor and the feeder to measure their pressures. The gas flow rates were controlled by using mass flow controllers (5850E, Brooks Instruments). After the reactor had been purged with  $\text{N}_2$ , 300 mL of an absorbent was injected, and the reactor then agitated. The stirring speed was limited to 50 rpm to keep the gas-liquid interface planar and smooth. To achieve a good gas-liquid contact, the gas was introduced into the top of the reactor. The absorption rates were calculated from the difference in the amounts of gas between the inlet and outlet. A ZRF model  $\text{CO}_2$  analyzer (Fuji Electric, 0-20 vol%) was used to measure the  $\text{CO}_2$  gas concentration at the reactor outlet.

## EXPERIMENTAL RESULT

### 1. Reaction Region Separation

If the reaction rate between AMP and  $\text{SO}_2/\text{NO}_2$  is fast pseudo-1st-order, like that of AMP/ $\text{CO}_2$ , the absorption rate of  $\text{SO}_2/\text{NO}_2$  can be determined by measurement of the gas partial pressure and absorption, according to reaction (28).

To determine  $m$ -order and  $n$ -order to distinguish the reaction region of  $\text{SO}_2/\text{AMP}$ , the absorption rate is measured with 3, 5, 10 and 15 kPa of  $\text{SO}_2$  and 10, 20 and 30 wt% of AMP at 313 K.

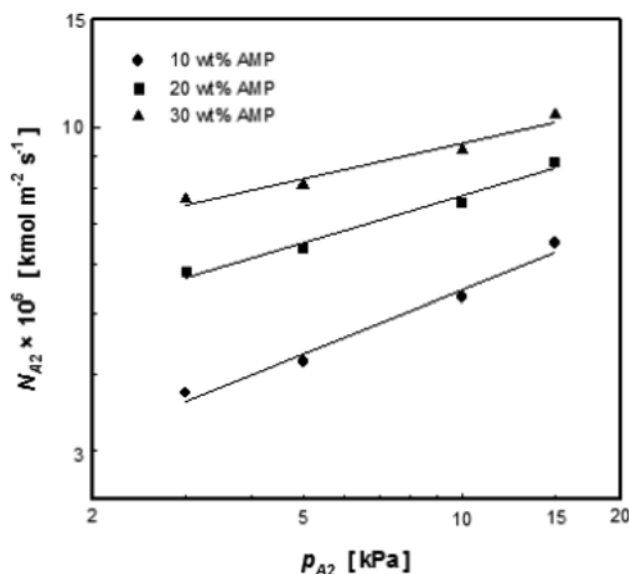


Fig. 2. Determination of m-order with respect to SO<sub>2</sub> partial pressure at different AMP concentrations and 313 K.

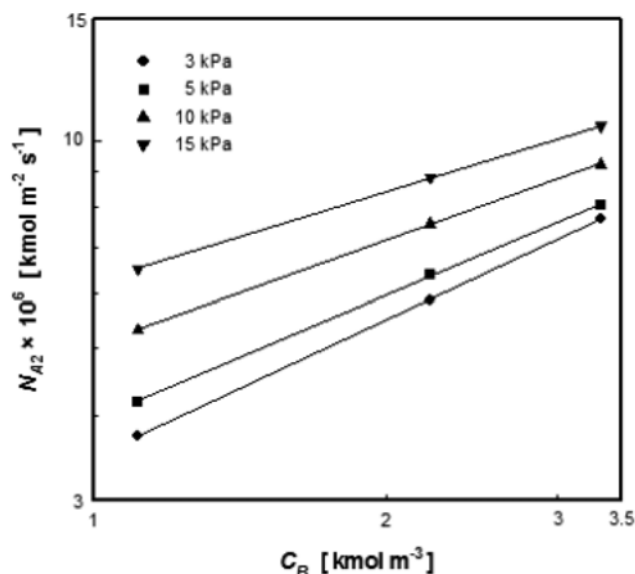


Fig. 4. Determination of m-order with respect to the AMP concentration at 313 K.

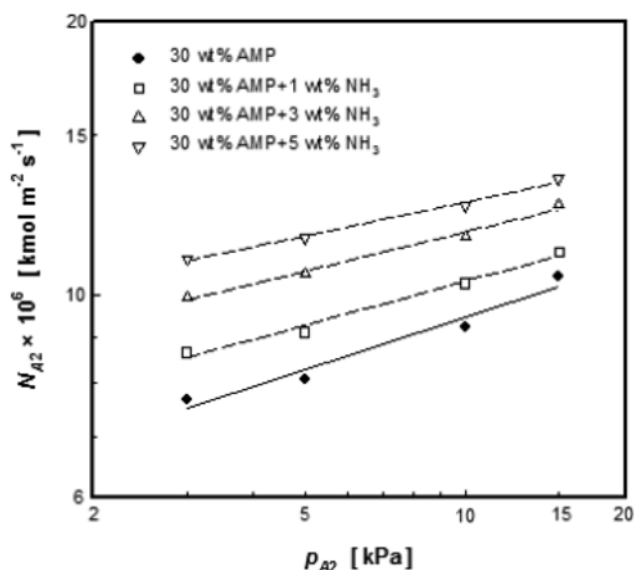


Fig. 3. Determination of m-order with respect to SO<sub>2</sub> partial pressure with different NH<sub>3</sub> concentrations at 313 K.

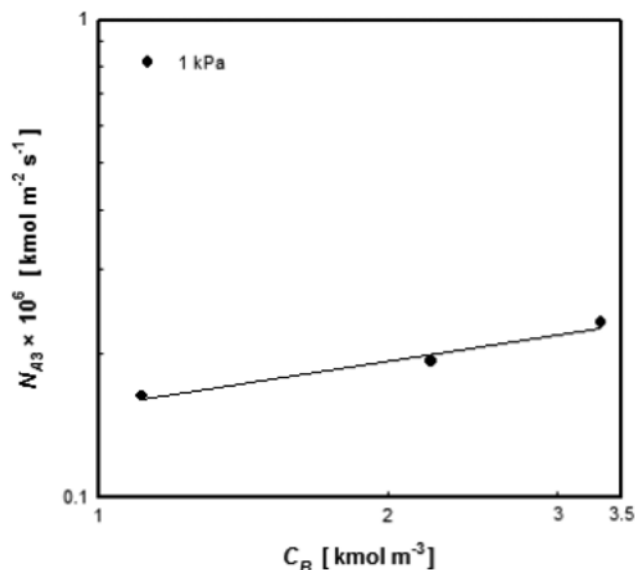


Fig. 5. Determination of n-order with respect to the AMP concentration at 313 K.

Fig. 2 shows a absorption rates between AMP solution and SO<sub>2</sub> as a function of the partial pressure of SO<sub>2</sub>; the slopes of these plots were 0.345, 0.251 and 0.192, with reaction orders,  $m$ , of  $-0.31$ ,  $-0.50$  and  $-0.62$  for 10, 20 and 30 wt% AMP, respectively.

Fig. 3, in addition, shows the absorption rates for 30 wt% AMP on the additions of 1, 3 and 5 wt% NH<sub>3</sub> as a function of the partial pressure of SO<sub>2</sub>, with slopes of 0.160, 0.143 and 0.124 and reaction orders,  $m$ , of  $-0.68$ ,  $-0.71$  and  $-0.75$ , respectively. Therefore, as seen in Figs. 2 and 3, a reaction region between SO<sub>2</sub> and AMP is decided not to fast pseudo-1st-order because  $m$  in reaction (28) from chapter 2 is not 1. As SO<sub>2</sub> absorbed in alkali solution also is widely known for very fast reaction with water like hydration, a reaction region between AMP and SO<sub>2</sub> is supposed to be an instan-

taneous reaction.

Fig. 4 shows an  $n$  reaction order for the absorption rate ( $N_{A2}$ ) and amine concentration, which involved diffusivity and physical solubility. As seen in Fig. 4, all the plots give straight lines, with slopes of 0.659, 0.600, 0.502 and 0.435 at 3, 5, 10 and 15 kPa, respectively. In the relation between concentration ( $C_B$ ) and absorption rate ( $N_{A2}$ ) for a 1st-order reaction, the slope of the plot by reaction equivalent ratio should be 0.5, but  $n$ -order for AMP concentration is not 1 for all pressure variables.

To find the  $m$ - and  $n$ -orders to distinguish the reaction region of NO<sub>2</sub>/AMP, the absorption rate was measured with an NO<sub>2</sub> partial pressure of 1 kPa and AMP concentrations of 10, 20 and 30 wt% at 313 K. An experiment to find the  $m$ -order was impossible because

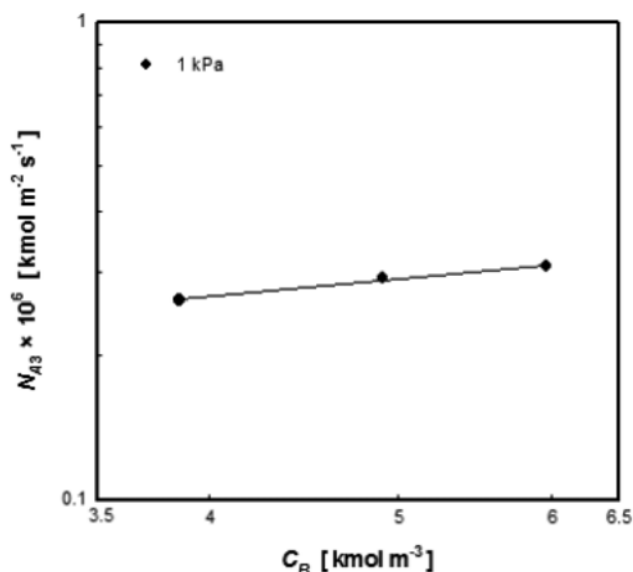


Fig. 6. Determination of n-order with respect to the concentration of  $\text{NH}_3$  added with 30 wt% AMP at 313 K.

of the low  $\text{NO}_2$  concentration, so the reaction follows an n-order. Therefore, an experimental n-order reaction for the absorption ( $N_{A3}$ ) and amine concentration ( $C_B$ ) was performed for the absorption reaction between the gas and liquid phase.

Figs. 5 and 6 show the absorption rates between 30 wt% AMP solution and  $\text{NO}_2$  with the addition of  $\text{NH}_3$  to the 30 wt% AMP solution to determine the n-order. As seen in Fig. 5 and Fig. 6, the plots give a straight line, with slopes of 0.3130 and 0.3777, respectively, with 30 wt% AMP on the addition of 1, 3 and 5 wt%  $\text{NH}_3$ . In the relation between the concentration ( $C_B$ ) and absorption rate ( $N_{A3}$ ) for a 1st-order reaction, the slope of the plot by reaction equivalent ratio should be 0.5, but the n-order is not 0.5 from this result. Therefore, the reaction region between  $\text{NO}_2$  and AMP is not fast 1st-order, but an instantaneous reaction.

## 2. Effect of $\text{NH}_3$ Addition

Absorption rate tests of the complex gas ( $\text{CO}_2/\text{SO}_2/\text{NO}_2$ ) into aqueous AMP containing  $\text{NH}_3$  as an additive were conducted under many conditions. The AMP concentrations were 10, 20 and 30 wt%, and those of the  $\text{NH}_3$  additive 1, 3 and 5 wt%. The absorption rates of  $\text{CO}_2/\text{SO}_2/\text{NO}_2$  were measured at an  $\text{NO}_2$  partial pressure of 1 kPa, and because of the low gas pressure in the cylinder, the effect of  $\text{NO}_2$  cannot be tested at high partial pressures. However, the experimental error is large and the experiment hard to conduct; therefore, the experiments with low partial pressure of  $\text{NO}_2$  were excluded from this study. Similarly to another test using a single gas, the phenomenon of resistance was disregarded at the gas-liquid interface, with the stirring speed limited to 50 rpm to maintain a planar and smooth gas-liquid interface.

To observe the effects of the concentration of the  $\text{NH}_3$  added to the AMP solution, the partial pressures of  $\text{CO}_2(p_{A1})$ ,  $\text{SO}_2(p_{A2})$  and  $\text{NO}_2(p_{A3})$  were fixed at 15, 1 and 1 kPa, respectively. Figs. 7 and 8 show the absorption rates of  $\text{CO}_2$  into aqueous AMP solutions as a function of the AMP (10, 20 and 30 wt%) and  $\text{NH}_3$  (1, 3 and 5 wt%) concentrations.

Fig. 7 shows the absorption rates as a function of the AMP con-

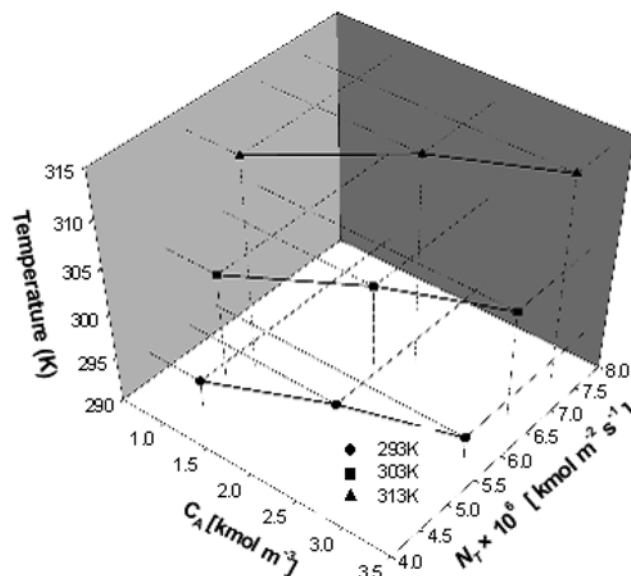


Fig. 7. The absorption rate of  $\text{CO}_2/\text{SO}_2/\text{NO}_2$  into aqueous AMP solution as a function of the AMP concentration (10, 20 and 30 wt%) at 303 K.

centration (10, 20 and 30 wt%). The simultaneous absorption rates of  $\text{CO}_2/\text{SO}_2/\text{NO}_2$  were  $4.51$  to  $5.42 \times 10^{-6}$ ,  $5.18$  to  $6.65 \times 10^{-6}$  and  $5.65$  to  $7.37 \times 10^{-6} \text{ kmol m}^{-2} \text{ s}^{-1}$ , respectively, and generally increased with increasing AMP concentration. As shown in Fig. 7, the increases in the rates of absorption as a function of temperature, presented in the Z axis, were smaller than those due to changes in the solution concentrations. This was a result of the promotion of mass transfer with increasing concentration gradient. Also, the absorption of  $\text{CO}_2/\text{SO}_2/\text{NO}_2$  into the absorbent causes increases the temperature, and therefore, increases the reaction rates, which is why the absorption rates increased.

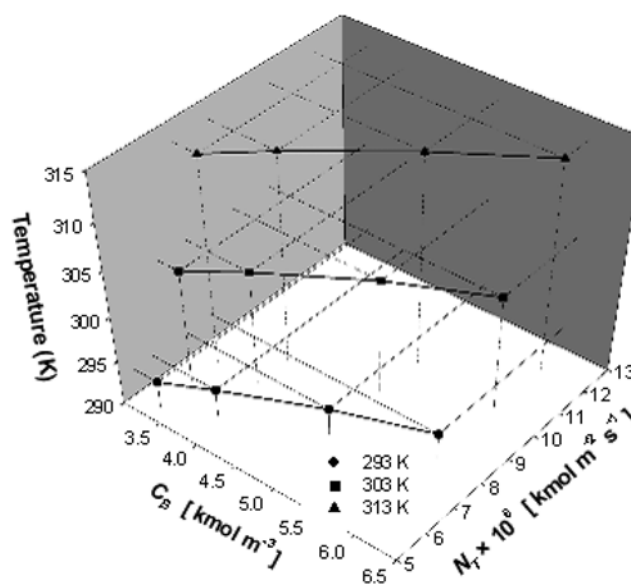


Fig. 8. The absorption rates of  $\text{CO}_2/\text{SO}_2/\text{NO}_2$  into aqueous AMP+ $\text{NH}_3$  solution as a function of the  $\text{NH}_3$  concentration (1, 3 and 5 wt%) at 303 K.

Fig. 8 compares the absorption rates of CO<sub>2</sub> into 30 wt% AMP on the addition of 1, 3 and 5 wt% NH<sub>3</sub> solution compared to that of 30 wt% AMP solution alone. On the addition of 1, 3 and 5 wt% NH<sub>3</sub>, the simultaneous absorption rates of CO<sub>2</sub>/SO<sub>2</sub>/NO<sub>2</sub> were 6.05 to 8.49×10<sup>-6</sup>, 7.16 to 10.41×10<sup>-6</sup> and 8.02 to 12.0×10<sup>-6</sup> kmol m<sup>-2</sup> s<sup>-1</sup>, respectively, increases of about 32.3 to 38.7% due to the addition of NH<sub>3</sub>. Also, the absorption rates increased with increasing temperature, but these variations were smaller than those with respect to concentration. However, on increasing the temperature, the range of variation also increased because the activation energy ( $E_{NH_3}$ ) of NH<sub>3</sub> is larger than that of AMP ( $E_{AMP}$ ); therefore, the contribution of NH<sub>3</sub> increases the absorption rates. The simultaneous absorption rates of CO<sub>2</sub>/SO<sub>2</sub>/NO<sub>2</sub> increased with concentration of solution, and that of CO<sub>2</sub> into the 30 wt% AMP solution with the addition of NH<sub>3</sub> was faster than that with AMP solution alone. Therefore, the addition of NH<sub>3</sub> increases the simultaneous absorption rates of CO<sub>2</sub>/SO<sub>2</sub>/NO<sub>2</sub> into AMP solution.

### 3. Effect of CO<sub>2</sub> Partial Pressure

Absorption rate tests of complex gas into aqueous AMP containing NH<sub>3</sub> as an additive were conducted under numerous conditions, with the influence of the CO<sub>2</sub> concentration observed. Figs. 9-10 show the absorption rates of CO<sub>2</sub> with respect to the AMP and NH<sub>3</sub> solution concentrations; the variables during these experiments were: NO<sub>2</sub> 1 kPa, AMP concentrations of 3, 5 and 10 wt%, 1 wt% NH<sub>3</sub> in 10 wt% AMP solution and CO<sub>2</sub> partial pressures of 5, 10 and 15 kPa.

Fig. 9 shows the absorption rates of the complex gas into solutions as a function of the CO<sub>2</sub> partial pressure. The absorption rates of CO<sub>2</sub>/SO<sub>2</sub>/NO<sub>2</sub> into 3-10 wt% AMP were 1.54 to 1.92×10<sup>-6</sup> and 3.83 to 4.87×10<sup>-6</sup> kmol m<sup>-2</sup> s<sup>-1</sup> at 5 and 15 kPa, respectively. As the AMP concentration and CO<sub>2</sub> partial pressure were increased, the absorption rates of the complex gas also increased. The absorption rate into 10 wt% AMP with the addition of NH<sub>3</sub> as a function of the CO<sub>2</sub> partial pressure (5-15 kPa) was 2.31 to 5.73×10<sup>-6</sup> kmol

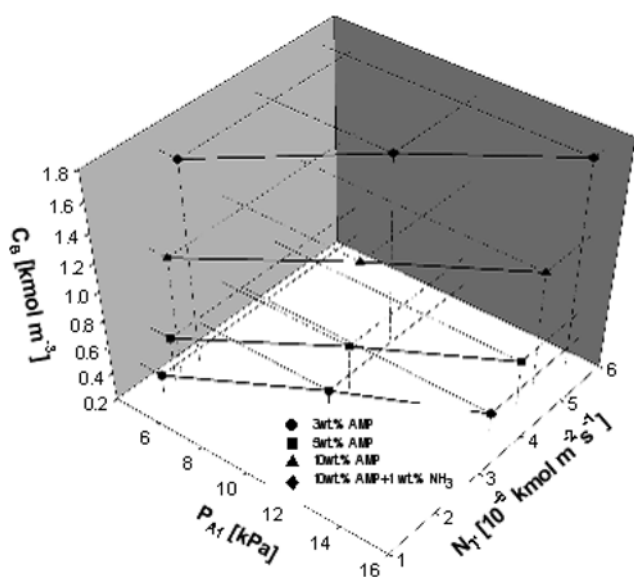


Fig. 9. The absorption rates of CO<sub>2</sub>/SO<sub>2</sub>/NO<sub>2</sub> into aqueous AMP and AMP+NH<sub>3</sub> solutions as a function of the pressure of CO<sub>2</sub> at 303 K.

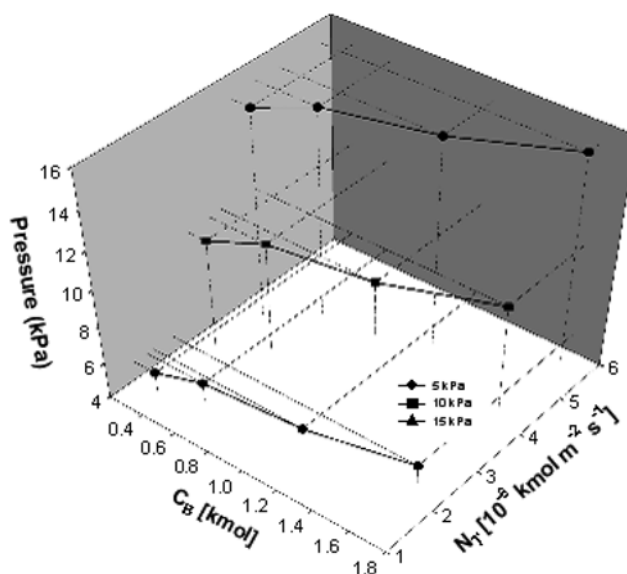


Fig. 10. The absorption rates of CO<sub>2</sub>/SO<sub>2</sub>/NO<sub>2</sub> into aqueous AMP and AMP+NH<sub>3</sub> solution as a function of the concentrations of AMP and NH<sub>3</sub> at 303 K.

m<sup>-2</sup> s<sup>-1</sup>. These results show that the increase in the absorption rate was higher than those at the partial pressures for SO<sub>2</sub> and NO<sub>2</sub>. In this case, NH<sub>3</sub> dominates the CO<sub>2</sub> in the reaction because the partial pressures of SO<sub>2</sub> and NO<sub>2</sub> were lower than 1 kPa. However, as a function of the partial pressure of SO<sub>2</sub>, because the partial pressure of SO<sub>2</sub> was relatively high, the NH<sub>3</sub> has an effect on the absorption of SO<sub>2</sub> into solution. Conversely, the absorption rates of SO<sub>2</sub> and NO<sub>2</sub> were almost uniform, but that of CO<sub>2</sub> was increased. Because the partial pressures of SO<sub>2</sub> and NO<sub>2</sub> were 1 kPa, which was lower than that of CO<sub>2</sub>, the absorption of SO<sub>2</sub> was dominated by a hydration reaction; therefore, SO<sub>2</sub> had no effect on the partial pressure of CO<sub>2</sub>.

Fig. 10 shows the absorption rate as a function of the partial pressure of CO<sub>2</sub> from the results in Fig. 9, showing increased absorption rates with increasing concentrations of AMP and NH<sub>3</sub>. In general, the simultaneous absorption rates of CO<sub>2</sub>/SO<sub>2</sub>/NO<sub>2</sub> were increased by increasing the partial pressure of CO<sub>2</sub>, as indicated on the Z axis, and the rate of increased with 10 wt% AMP+1 wt% solution more than with 10 wt% AMP solution alone. Therefore, the addition of NH<sub>3</sub> into AMP solution is an effective means of enhancing the absorption rates of blended gases.

### 4. Effect of SO<sub>2</sub> Partial Pressure

To estimate the effects of the SO<sub>2</sub>( $p_{A2}$ ) partial pressures and NH<sub>3</sub> additive concentrations in 30 wt% AMP solution, the partial pressures of CO<sub>2</sub>( $p_{A1}$ ) and NO<sub>2</sub>( $p_{A3}$ ) were fixed at 15 and 1 kPa, respectively. Figs. 11-12 show the absorption rates of CO<sub>2</sub> into aqueous AMP solution as a function of the SO<sub>2</sub> partial pressure (1, 3 and 5 kPa) with 10 wt% AMP solution and NH<sub>3</sub> additive concentrations of 1, 3 and 5 wt%.

Fig. 11 shows the absorption rates of the blended gas into the AMP solution as a function of the SO<sub>2</sub> partial pressure. The absorption rates of CO<sub>2</sub>/SO<sub>2</sub>/NO<sub>2</sub> into 3-10 wt% AMP solution were 3.83 to 4.87×10<sup>-6</sup> and 4.82 to 5.82×10<sup>-6</sup> kmol m<sup>-2</sup> s<sup>-1</sup> at 1 and 5 kPa, respectively, and increased as the AMP concentration and SO<sub>2</sub> partial pres-

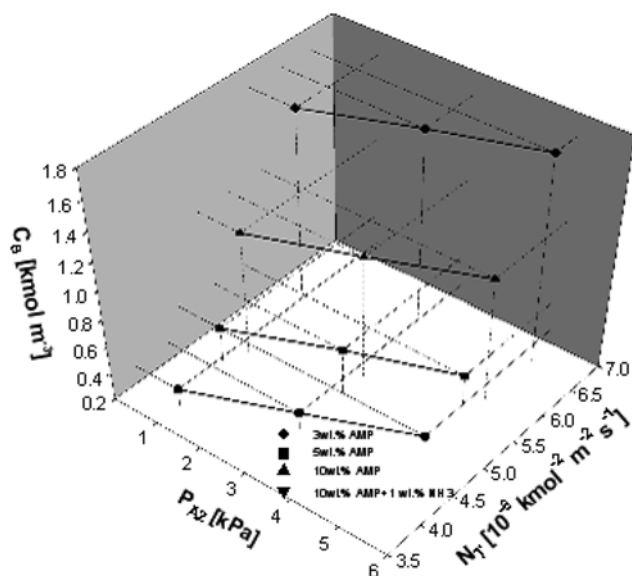


Fig. 11. The absorption rates of  $\text{CO}_2/\text{SO}_2/\text{NO}_2$  into aqueous AMP and AMP+ $\text{NH}_3$  solutions as a function of the partial pressure of  $\text{SO}_2$  at 303 K.

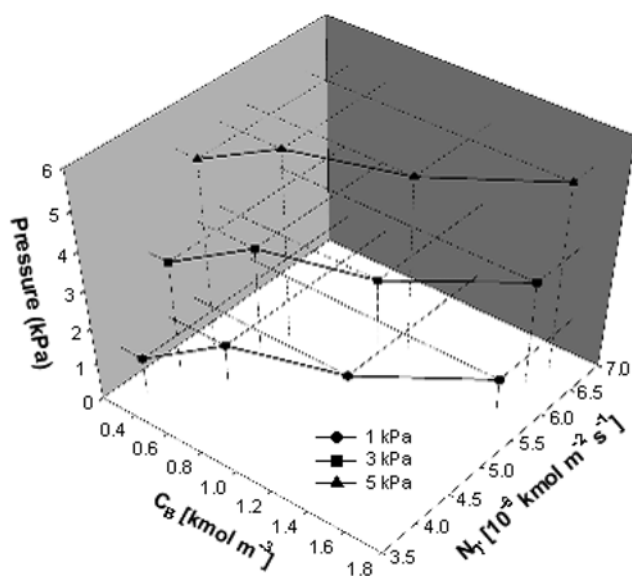


Fig. 12. The absorption rates of  $\text{CO}_2/\text{SO}_2/\text{NO}_2$  into aqueous AMP and AMP+ $\text{NH}_3$  solutions as a function of the AMP and  $\text{NH}_3$  concentrations at 303 K.

sure increased. This resulted from the increased concentration gradient with increasing amount of  $\text{SO}_2$  absorbed at the gas-liquid interface. On increasing the concentration of the  $\text{NH}_3$  addition (1, 3 and 5 wt%), the simultaneous absorption rates of  $\text{CO}_2/\text{SO}_2/\text{NO}_2$  ranged from  $5.73$  to  $6.64 \times 10^{-6} \text{ kmol m}^{-2} \text{ s}^{-1}$ , increases of about 12.4–15.0% for the range of  $\text{SO}_2$  partial pressures (1, 3 and 5 kPa).

Fig. 12 shows the absorption rates as a function of the partial pressure of  $\text{SO}_2$  from the results in Fig. 9, showing increases with increasing concentrations of AMP and  $\text{NH}_3$ . Also, the increased rate with 10 wt% AMP solution and the addition of 1 wt%  $\text{NH}_3$  was higher than that with 10 wt% AMP solution alone, so the addition of  $\text{NH}_3$

into 10 wt% AMP solution was effective in enhancing the absorption rates of blended gases.

## CONCLUSION

$\text{NH}_3$  solution was added to aqueous AMP solution for the simultaneous absorption of  $\text{CO}_2/\text{SO}_2/\text{NO}_2$ . The absorption rate of  $\text{CO}_2/\text{SO}_2/\text{NO}_2$  into the aqueous blended amine solutions was investigated by using a stirred cell reactor. The reaction region between  $\text{SO}_2/\text{NO}_2$  and AMP was not fast 1st-order but an instantaneous reaction. The  $\text{NH}_3$  additive concentrations to the 10 wt% AMP solution were 1, 3 and 5 wt%. The absorption rates of  $\text{CO}_2/\text{SO}_2/\text{NO}_2$  into a blend of AMP and  $\text{NH}_3$  as a function of temperature were 32.3 to 38.7% higher than with of AMP alone. The simultaneous absorption rates of  $\text{CO}_2/\text{SO}_2/\text{NO}_2$  into aqueous AMP+ $\text{NH}_3$  solution ranged from  $3.83$  to  $4.87 \times 10^{-6} \text{ kmol m}^{-2} \text{ s}^{-1}$  at 15 kPa, which was increased by 15.0 to 16.9% than with 30 wt% AMP solution alone. This means that  $\text{NH}_3$  solution could act as an alternative control for  $\text{CO}_2/\text{SO}_2/\text{NO}_2$  from a flue gas due to its high absorption capacity and fast absorption rate.

## ACKNOWLEDGEMENTS

This research was supported for two years by Pusan National University Research Grant and the Brain Korea 21 Project in 2010.

## REFERENCES

1. UNFCCC, Kyoto Protocol to the United Nations Framework Convention on Climate Change, FCCC/CP/1997/L.7/Add.1, Bonn (1997).
2. IPCC (Intergovernmental Panel on Climate Change), Policymaker's Summary of the Scientific Assessment of Climate Change, Report to IPCC from Working Group, Branknell, UK: Meteorological Office (1990).
3. H. M. Um, The Study on the Development of Demo Plant Scale Carbon Dioxide Separation and Conversion Technologies in Power Station, 2000-C-CD02-P-01, Korea (2003).
4. A. B. Rao and E. S. Rubin, *Environ. Sci. Technol.*, **36**, 4467 (2002).
5. B. P. Mandal, A. K. Biswas and S. S. Bandyopadhyay, *Chem. Eng. Sci.*, **58**, 4137 (2003).
6. B. P. Mandal and S. S. Bandyopadhyay, *Chem. Eng. Sci.*, **61**, 5440 (2006).
7. P. V. Danckwerts, *Chem. Eng. Sci.*, **34**, 443 (1979).
8. M. Caplow, *J. Am. Chem. Soc.*, **90**, 6795 (1968).
9. P. M. M. Blauwhoff, G. F. Versteeg and W. P. M. van Swaaij, *Chem. Eng. Sci.*, **38**, 1411 (1983).
10. B. P. Mandal, A. K. Biswas and S. S. Bandyopadhyay, *Chem. Eng. Sci.*, **58**, 4137 (2003).
11. A. K. Chakraborty, G. Astarita and K. B. Bischoff, *Chem. Eng. Sci.*, **41**, 997 (1986).
12. H. L. Bai and A. C. Yeh, *Ind. Eng. Chem. Res.*, **36**, 2490 (1997).
13. Y. F. Diao, X. Y. Zheng, B. S. He, C. H. Chen and X. C. Xu, *Energy Convers. Manage.*, **45**, 2283 (2004).
14. J. T. Yeh, K. P. Resnik, K. Rygle and H. W. Pennline, *Fuel Process. Technol.*, **86**, 1533 (2005).
15. H. Hikita, S. Asai and H. Nose, *AIChE J.*, **24**, 147 (1978).

16. H. Hikita, S. Asai and T. Tsufi, *AIChE J.*, **23**, 538 (1977).
17. B. He, X. Zheng, Y. Wen, H. Tong, M. Chem and C. Chen, *Energy Convers. Manage.*, **44**, 2175 (2003).
18. S. M. Yih and K. P. Shen, *Ind. Eng. Chem. Res.*, **27**, 2237 (1988).
19. A. K. Saha, S. S. Bandyopadhyay and A. K. Biswas, *Chem. Eng. Sci.*, **50**, 3587 (1995).
20. C. Alvarez-Fuster, N. Midoux, A. Laurent and J. C. Charpentier, *Chem. Eng. Sci.*, **35**, 1717 (1980).
21. W. J. Choi, B. M. Min, J. B. Seo, S. W. Park and K. J. Oh, *Ind. Eng. Chem. Res.*, **48**, 4022 (2009).